

# Effect of Anisotropy on SAW Behavior in LGS Orientation with Euler Angles ( $0^\circ$ , $22^\circ$ , $90^\circ$ )

Natalya Naumenko<sup>1,2</sup>

<sup>1)</sup> Moscow Technical University of Communication and Information

<sup>2)</sup> Moscow Steel and Alloys Institute

[nnaumenko@ieee.org](mailto:nnaumenko@ieee.org)

**Abstract** — The nature of spurious responses observed experimentally in admittance function of SAW resonator on LGS cut with Euler angles ( $0^\circ$ ,  $22^\circ$ ,  $90^\circ$ ) is investigated. The resonator characteristics were found to be very sensitive to deviation of propagation direction from the required angle because of dramatically increasing interaction between SH and Rayleigh modes, in this LGS orientation. Analysis of velocity dispersion in the grating and visualization of acoustic fields associated with two SAW modes revealed the mechanism of interaction between the modes and the ways of reducing the effect of this interaction on resonator performance.

## I. INTRODUCTION

Langasite  $\text{La}_3\text{Ga}_5\text{SiO}_{14}$  (LGS) is one of few materials with similar crystal structure, which can be used as a substrate in wireless SAW sensors with resonator-type structure operating in a wide range of temperatures, up to  $700^\circ\text{C}$ , due to successful combination of low acoustic propagation losses, sufficiently high electromechanical coupling factor, high melting point and absence of phase transitions. Today there is a strong demand for such sensors in automotive industries [1].

For high-temperature applications orientations with low temperature coefficient of frequency (TCF) are preferable, whereas resonator-type structure requires sufficiently high electromechanical coupling. Only few cuts of LGS combine zero TCF and high coupling. One of them is characterized by the Euler angles ( $0^\circ, 22^\circ, 90^\circ$ ) and refers to symmetric orientations, in which shear horizontally (SH) polarized bulk acoustic wave (BAW) is modified by the piezoelectric effect into the quasi-bulk Bluestein-Gulyaev wave (BGW). This orientation was reported [2] as a good choice for high temperature SAW sensors with resonator structure.

With increasing electrode thickness BGW becomes better localized near the surface and its electromechanical coupling grows. Application of heavy electrode material, such as platinum (Pt), helps to increase the reflection coefficient and produce SAW resonators on LGS with higher quality factors. Besides, Pt provides low resistivity at high temperatures and good adhesiveness of metallic layer to the substrate [3].

The sensitivity of BGW to variation of electrode thickness enables high coupling when electrodes are sufficiently thick but it may be also a drawback for manufacturing SAW resonators with stable electrical parameters. Another specific feature of LGS cut ( $0^\circ, 22^\circ, 90^\circ$ ), which was recently observed experimentally [4], is a high sensitivity to misorientation of propagation direction on a substrate. It is much higher than in

other BGW cuts and results in splitting of the main resonance into few resonances and degradation of resonator performance when even small deviation of propagation direction occurs because of technological errors or defects of crystal structure.

This work is aimed at clarifying the nature of theoretically and experimentally observed spurious modes via analysis of anisotropy and its effect on the behavior of BGW in LGS cut ( $0^\circ$ ,  $22^\circ$ ,  $90^\circ$ ) and in periodic metal gratings built on this cut.

## II. BGW AND RAYLEIGH SAW IN LGS CUTS ( $0^\circ$ , $\theta$ , $90^\circ$ )

LGS refers to the point symmetry class 32, which is characterized by three two-fold symmetry axes, one of which is parallel to the crystal axis X. For SAW propagating in orientations with Euler angles ( $0^\circ$ ,  $\theta$ ,  $90^\circ$ ), the sagittal plane coincides with YZ plane of crystal, in which all displacements are uncoupled with electric fields. Therefore, only quasi-bulk BGW polarized along X axis may have nonzero electromechanical coupling while Rayleigh SAW is piezoelectrically uncoupled.

Fig.1 shows the velocities of two modes and TCF of BGW, as functions of angle  $\theta$ . All calculations were made with LGS constants reported in [5]. With these constants, BGW is characterized by zero TCF when  $\theta \approx 22^\circ$ . In the same orientation, two modes propagate with nearly equal velocities.

If the resonator structure is strictly positioned on SAW wafer to provide SAW propagation perpendicular to X-axis, as described by the Euler angles ( $0^\circ, 22^\circ, 90^\circ$ ), then Rayleigh wave is uncoupled with BGW and has no effect on the device performance. In case of inaccurate positioning of resonator structure on the substrate, the electromechanical coupling of Rayleigh SAW grows and the interaction between SAW and BGW degrades resonator performance. In general, any perturbation of the substrate symmetry eliminates degeneracy and causes interaction between two modes.

With deviation of the third Euler angle from  $90^\circ$ , Rayleigh wave transforms into leaky SAW and the two-partial BGW solution modifies into the four-partial SAW. Fig.2 shows the velocities of two modes and attenuation of leaky SAW in orientations with Euler angles ( $0^\circ$ ,  $22^\circ$ ,  $90^\circ + \psi$ ), as functions of angle  $\psi$ . Within the analyzed interval of angles  $\psi$ , SAW mode arising from BGW stays quasi-bulk, and its velocity is close to that of the limiting BAW propagating along the crystal surface. The displacement vectors of both SAW modes rotate rapidly with increasing angle  $\psi$ , which means potentially strong coupling between the modes, in SAW resonators.

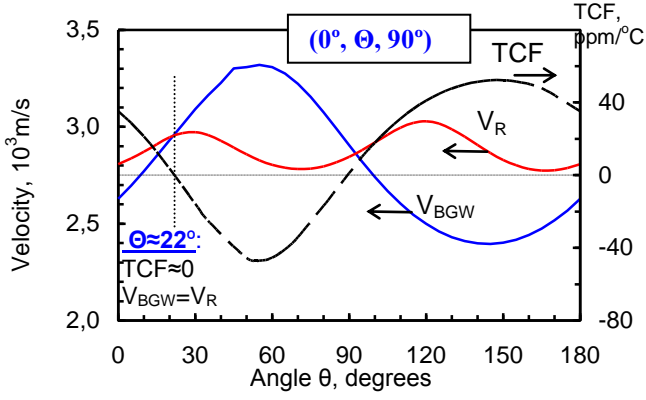


Fig.1. Velocities of Rayleigh SAW and BGW and TCF of BGW, in LGS orientations with Euler angles  $(0^\circ, \theta, 90^\circ)$ , as functions of angle  $\theta$ . Simulations were made with constants reported in [5].

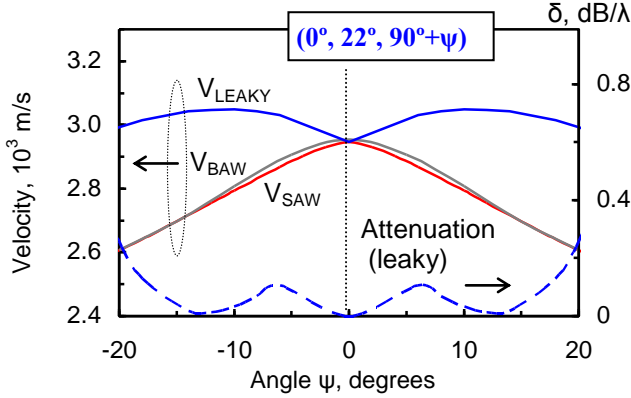


Fig.2. Velocities of two modes propagating in LGS orientations with Euler angles  $(0^\circ, 22^\circ, 90^\circ+\psi)$ , as functions of angle  $\psi$ . Grey lines show the velocity of the limiting SH-BAW.

To understand the nature of multiple resonances in the admittance function of SAW resonators on LGS cut  $(0^\circ, 22^\circ, 90^\circ)$ , the effect of anisotropy on resonator characteristics was analyzed using a combination of previously developed numerical techniques: method *SDA-FEM-SDA* [6] with upper subspace specified as the air, the *rational approximation of admittance* of the grating [7], which has been recently applied to analysis of interaction between SAW modes in LGS cut  $(0^\circ, 138.5^\circ, 26.6^\circ)$  [8], and visualization of acoustic fields using *extended version of SDA-FEM-SDA* [9].

### III. ANALYSIS OF RESONATOR CHARACTERISTICS

Fig. 3a shows the calculated dispersion of SAW velocity in Pt grating on LGS cut  $(0^\circ, 22^\circ, 90^\circ)$ . The normalized electrode thickness is  $h/\lambda=1\%$ . The velocities are shown as functions of the normalized frequency  $f'=fp/V_{BAW}$ , where  $p$  is the periodicity of the grating and  $V_{BAW}=2963.9$  m/s is the velocity of SH-polarized BAW.

Two electrical boundary conditions were considered, open circuit (OC) and short circuit (SC). The ratio of two dispersion curves determines the admittance of SAW resonator (Fig. 3b). The resonance and anti-resonance occur at the lower edge of the stopband determined for SC and OC gratings, respectively.

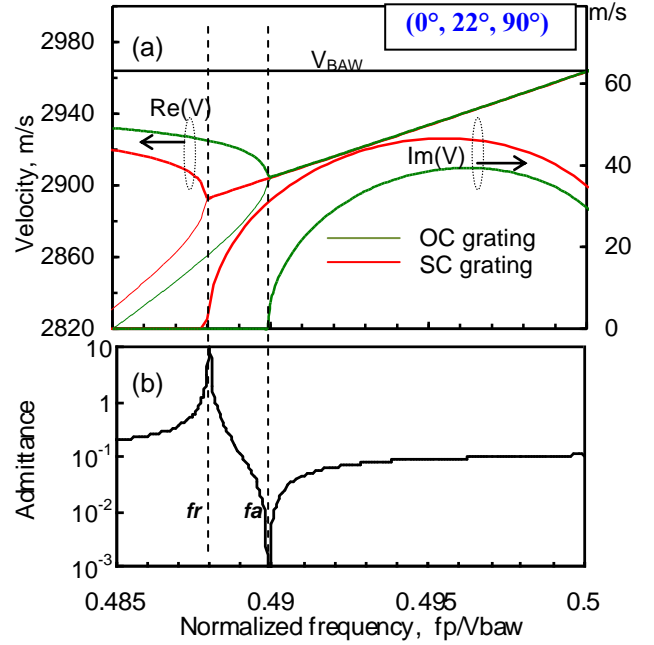


Fig.3. Velocity (a) and admittance (b), as functions of normalized frequency, in SC and OC platinum gratings on LGS cut  $(0^\circ, 22^\circ, 90^\circ)$ . Normalized electrode thickness is  $h=1\%/\lambda$ . Thinner lines refer to backward propagating modes in the gratings. Dashed vertical lines indicate resonant and anti-resonant frequencies.

With the third Euler angle different from  $90^\circ$ , the admittance shows two spurious responses, which degrade the resonator performance, even when the deviation of the third Euler angle is about  $0.1^\circ$ . If it is  $0.5^\circ$ , then one resonance is replaced by three comparable resonances. The nature of spurious resonances can be understood from velocity dispersion in LGS  $(0^\circ, 22^\circ, 91^\circ)$  with Pt grating, which is shown in Fig. 4a, and the admittance function (Fig. 4b).

Assuming that the resonant frequency associated with BGW does not shift noticeably compared to orientation  $(0^\circ, 22^\circ, 90^\circ)$  (Fig. 3a), the second resonance in Fig. 4b,  $fr_2=0.4887$ , can be referred to the lower edge of the SC stopband built by interaction between the counter propagating BGWs. The first and the third resonances occur at the edges of the new stopband built by interaction between the counter-propagating Rayleigh-type waves, because this wave is piezoelectrically coupled in  $(0^\circ, 22^\circ, 91^\circ)$  cut. At the frequency slightly higher than the second resonance, maximum interaction between two waves is expected.

These assumptions about the nature of three resonances in Fig. 4b agree with the behavior of squared dispersion parameter,  $D^2$ , where  $D=(p/\lambda-0.5)$ , calculated as function of the normalized frequency  $f'$ , for each of two modes (Fig. 4c). The red and blue lines, which refer to BGW and Rayleigh-type wave, respectively, are nearly parabolic though perturbed by interaction between the modes.

As shown in Fig. 5, with further increasing of the third Euler angle the reflection coefficient of Rayleigh-type wave grows and the resonator performance is built mostly by this

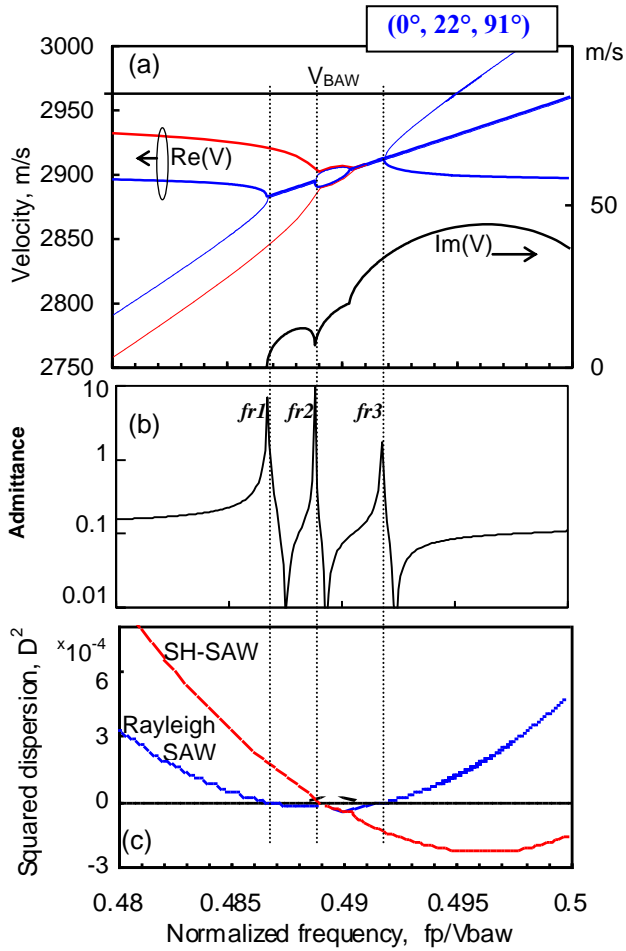


Fig.4. Velocity (a) , admittance (b) and squared dispersion parameter (c) as functions of normalized frequency, in SC platinum grating on LGS cut ( $0^\circ, 22^\circ, 91^\circ$ ). Normalized electrode thickness is  $h/\lambda=1\%$ . Dashed line in (c) refers to imaginary part of  $D^2$

wave while the modified BGW behaves as spurious mode. The calculations refer to LGS orientation ( $0^\circ, 22^\circ, 95^\circ$ ). Two resonances of the admittance calculated at synchronous resonance condition,  $\lambda=2p$ , obviously refer to Rayleigh-type SAW. The first resonance is much better pronounced than the second one. However, with detuning from the synchronous resonance condition (e.g. in short resonators) one more spurious resonance can degrade the resonator characteristics.

#### IV. VISUALIZATION OF THE WAVE STRUCTURE

The nature of the waves propagating in SAW resonators can be better understood from the plots visualizing mechanical displacements, which follow wave propagation. The method of calculating displacement fields in the grating was described in [8], where acoustic modes were investigated in two cuts of lithium niobate with  $SiO_2$  overlay. Fig.6a,c show the structure of two modes propagating in LGS cut ( $0^\circ, 22^\circ, 91^\circ$ ) at low frequency, when both waves are unperturbed by interactions with each other and with the grating. One of the waves is quasi-bulk, with the wave front tilted by about  $18^\circ$  with respect to the surface, which agrees with the wave vector of the limiting SH-polarized BAW shown on the slowness

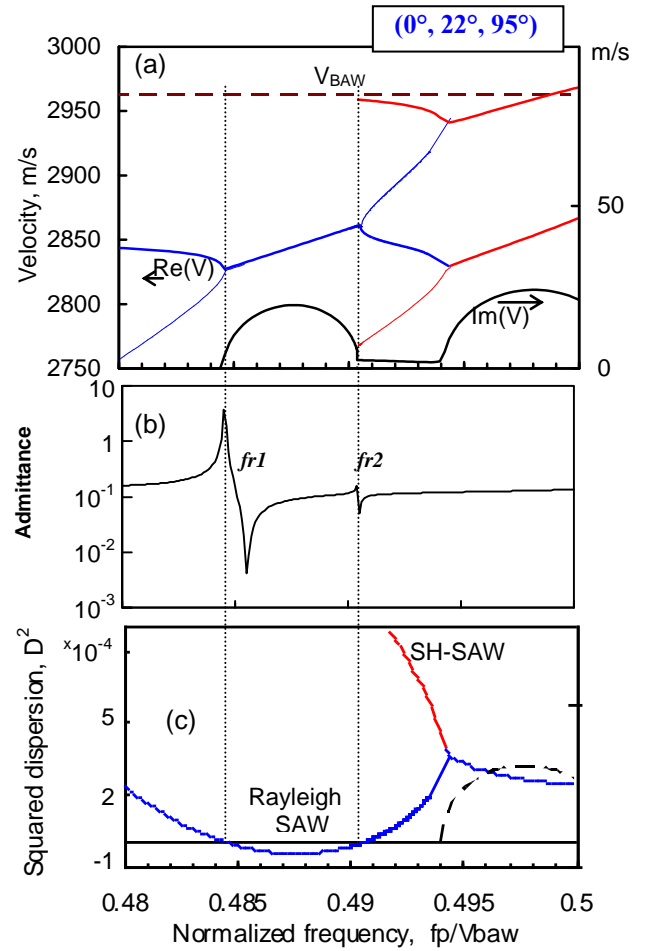
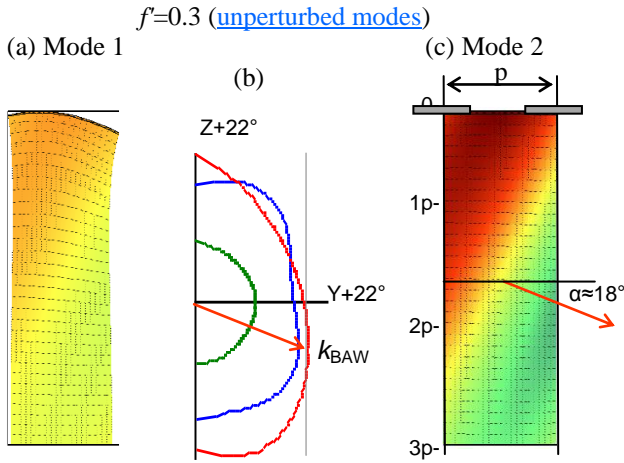


Fig.5. Velocity (a) , admittance (b) and squared dispersion (c) as functions of normalized frequency, in SC platinum grating on LGS cut ( $0^\circ, 22^\circ, 95^\circ$ ). Normalized electrode thickness is  $h/\lambda=1\%$ . Dashed line in (c) refers to imaginary part of  $D^2$

surface (Fig. 6b). The lower velocity mode is Rayleigh-type wave, with displacement mostly confined in the sagittal plane.

With frequency increasing and approaching the first resonance,  $fr1$ , interaction between two SAW modes modifies their structure. According to Fig.4, the first resonance occurs on the lower velocity (Rayleigh-type) branch, but the wave has mixed polarization (Fig.6d) because of this interaction. At the second ( $fr2$ , Fig.6e) and third ( $fr3$ , Fig. 6f) resonances, SH-polarization component stays nearly constant but interaction between the modes results in the fast variation of displacements in the sagittal plane with frequency.

The high sensitivity of BGW to misorientation of the propagation direction in LGS cut ( $0^\circ, 22^\circ, 90^\circ$ ) is illustrated in Fig.7. With thin or light electrodes, the wave structure and hence the resonator performance change dramatically with misorientation (Fig.7a). The sensitivity is still high when Pt thickness is  $1\% \lambda$  (Fig.7b) but when it is about  $2.5\% \lambda$ , the wave looks as well-behaved BGW, with the structure slowly varying with misorientation. In this case, interaction between two SAW modes can be ignored. It should be mentioned that in LGS cut ( $0^\circ, 10^\circ, 90^\circ$ ), for example, low sensitivity to misorientation is observed for any electrode thickness.



Modes perturbed by interactions in the grating:

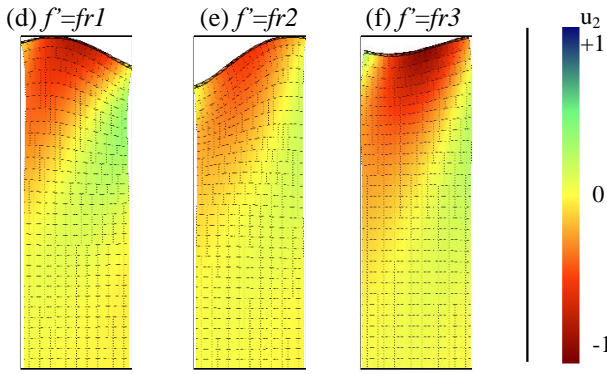


Fig.6. Mechanical displacements caused by wave propagation in LGS,  $(0^\circ, 22^\circ, 91^\circ)$  with Pt grating ( $h/\lambda=1\%$ ), as functions of propagation direction (horizontal axis) and depth (vertical axis), shown as deformation of regular grid, in the sagittal plane, and colored diagrams, as amplitudes in shear horizontal direction: (a),(c) unperturbed modes at low frequency; (d)-(f) perturbed modes analyzed at three resonant frequencies. Slowness surface (b) explains the tilt of SH-BAW (red) wave vector,  $k_{BAW}$ , into the bulk.

## V. CONCLUSION

LGS cut with Euler angles  $(0^\circ, 22^\circ, 90^\circ)$  was found to be very sensitive to misorientation of the propagation direction on a wafer. Any misorientation is followed by fast degradation of resonator performance. This effect can be reduced by increasing of electrode thickness or changing of cut angle.

## REFERENCES

- [1] S. Ballandras, W. Daniau, G. Martin, and P. Berthelot, "Wireless Temperature Sensor using SAW Resonators for Immersed and Biological Applications", in *Proc. IEEE Ultrason. Symp.* 2002, pp.445-448.
- [2] E. Berkenpas, S. Bitla, P. Millard, and M. Pereira da Cunha, "Pure Shear Horizontal SAW Biosensor on Langasite", *IEEE Trans. UFFC-51*, 2004, pp.1404-1411.
- [3] J.A. Thiele, and M. Pereira da Cunha, "Platinum and Palladium High-Temperature Transducers on Langasite", *IEEE Transactions UFFC*, 2005, vol. 52, no. 4, pp. 545-549.
- [4] S. Sakharov, N. Naumenko, A. Zabelin and S. Zhgoon, Characterization of langasite for application in high temperature SAW sensors, to be published in *Proc. IEEE Ultrasonics Symp.*, 2011.

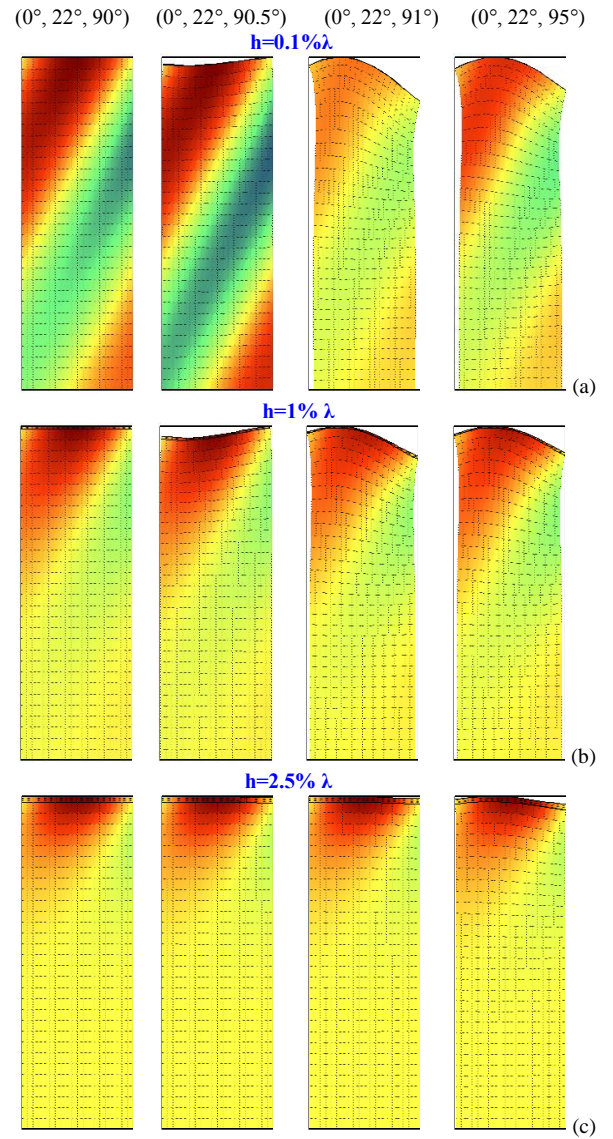


Fig.7. Mechanical displacements caused by wave propagation in LGS cuts with Pt grating: (a)  $h=0.1\%$ , (b)  $h=1\%$ , (c)  $h=2.5\%$ . Calculations were made at the first resonant frequency.

- [5] A.Bungo, C.Jian, K.Yamaguchi, Y.Sawada, S.Uda, and Yu. Pisarevsky, "Analysis of surface acoustic wave properties in the rotated Y-cut langasite Substrate", *Jpn. J.Appl.Phys.*, 1999, v.38, pp.3239-3243.
- [6] N. F. Naumenko, " A Universal Technique for Analysis of Acoustic Waves in Periodic Grating Sandwiched Between Multi-Layered Structures and Its Application to Different Types of Waves", *Proc. 2010 IEEE Ultrasonics Symposium*, pp. 1673-1676, 2010.
- [7] N. F. Naumenko, and B. P. Abbott, "Fast numerical technique for simulation of SAW dispersion in periodic gratings and its application to some SAW materials", in *Proc. IEEE Ultrason. Symp.*, 2007, pp.166-170.
- [8] N. F. Naumenko, "Analysis of Interaction Between Two SAW Modes in Pt Grating on Langasite Cut  $(0^\circ, 138.5^\circ, 26.6^\circ)$ ", *IEEE Transactions UFFC*, 2011, vol. 58, no. 11.
- [9] N.F.Naumenko, and B.P.Abbott, "Transformation of Acoustic Waves in Periodic Metal Grating Sandwiched Between Piezoelectric and Dielectric ", *IEEE Transactions UFFC*, 2011, vol. 58, no. 10, pp.2181-2187.